

Innovations in the design of mechanical components for a beamline - The SRI'95 Workshop 2 Summary

T. M. Kuzay, and T. Warwick*

Experimental Facilities Division, Advanced Photon Source, Argonne National Laboratory, Argonne, Illinois 60439

**Advanced Light Source, Lawrence Berkely Laboratory, Berkeley, CA 94720*

(Presented on 12 October 1995)

The Synchrotron Radiation Instrumentation 1995 Conference (SRI'95) was hosted by the Advanced Photon Source (APS) at Argonne National Laboratory (ANL). Of the many workshops within the conference, the SRI'95 Workshop 2 was "Innovations in the Design of Mechanical Components of a Beamline." The workshop was attended well with over 140 registrants. The following topics were discussed. Industry's perspective on the status and future was provided by Huber Diffractiontechnik, Oxford Instruments, and Kohzu Seiko Ltd. on goniometers/diffractometers, advanced manufacturing technique of high heat load components, such as the APS photon shutter, and the specialties of monochromators provided to the third-generation synchrotrons, respectively. This was followed by a description of the engineering of a dual function monochromator design for water-cooled diamond or cryogenically cooled silicon monochromators by CMC CAT/APS. Another category was the nagging problem of sensitivity of the photon beam position monitors (XBPM) to bending magnet radiation ("BM contamination") and the undulator magnet gap changes. Problem descriptions and suggested solutions were provided by both the Advanced Light Source (ALS) and the APS. Other innovative ideas were the cooling schemes (enhanced cooling of beamline components using metallic porous meshes including cryo-cooled applications); Glidcop photon shutter design using microchannels at the ALS; and window/filter design, manufacture and operational experiences at CHESS and PETRA/HASYLAB. Additional discussions were held on designing for micromotions and precision in the optical support systems and smart user filter schemes. This is a summary of the presentations at the Workshop. © 1995 American Institute of Physics

I. THE MORNING SESSION

Martin Townsend from Oxford Industries, England, discussed special manufacturing and joining techniques used in the manufacture of the APS front-end and beamline components. A case in point was the design and manufacturing innovations used in the APS photon shutter. This device handles heat flux levels of about 600 W/mm² in normal incidence with a total power of 6 kW from undulator A in the current phase of APS operations at 100-mA and 7-GeV. Design features include full UHV compatibility (10⁻¹¹ Torr vacuum levels); no vacuum-coolant joint; fail-safe design; replaceable absorber plate (either in consideration of replacement for maintenance or for 300-mA operations in the future); cooled containment against the reflected/scattered radiation; enhanced heat transfer in cooling; and good engineering safety in materials. The enhanced heat transfer technique is used to obtain an operational heat transfer coefficient of 3 W/cm²K using porous copper mesh in the coolant channels. The deionized water flow rate is about 1.0 gpm per channel resulting in a total deionized water requirement of about 5.0 gpm per unit. While very efficient, the porous mesh also results in vibration-free performance with no erosion/corrosion concerns.

The absorber plate itself is OFHC copper faced with a 3-mm-thick Glidcop plate for high temperature/stress operations. The two plates are explosion bonded as is the

transition section from the OFHC copper to the stainless steel flange over the articulated coolant entry end. An additional manufacturing novelty was in the design of the nocoolant vacuum joint. To achieve this, an OFHC copper plate almost one meter long was gundrilled with seven dead-ended 9-mm-diameter coolant holes. About 98 cm down, the holes for the seven channels were cross cut joining them laterally for the internal return of the coolant water. Electro discharge machining (EDM) was used in the cross cutting. This new technique, which is applicable at such depths, opens up new opportunities in the design of a variety of beamline components (including optics) to achieve no-coolant vacuum joints in HV/UHV operations.

So that the copper mesh inserts fit closely into the cooling channels, they were produced by the APS and issued to Oxford. The brazing of copper mesh to OFHC, Glidcop/OFHC, and Glidcop/SS using silver braze compound had to be researched and developed to accomplish the brazing needs in a variety of beamline components for the APS. Determining the length of the heating/cooling cycles and close monitoring of temperature profiles in the vacuum furnace were extensively studied under laboratory conditions. These APS developments were transferred to Oxford and to its subcontractors. However, vendor representatives concluded that, while excellent support was provided by the APS, transferring laboratory processes to larger scale manufacturing processes was still a problem. The time

RECEIVED
MAR 27 1996
OSTI

DISTRIBUTION OF THIS DOCUMENT IS UNLIMITED

MASTER

DISCLAIMER

Portions of this document may be illegible in electronic image products. Images are produced from the best available original document.

pressure to meet tight schedules did not provide the vendor with enough in-house development time.

Norman Huber (with coauthors, Georg Kotter and Rudolf Heilmair) from Huber-Diffraktionstechnik GMBH, Germany, gave an excellent presentation on the present and future of goniometer designs. Diffractometers, goniometers, and optical stages are constantly being challenged by the ever increasing demand by the users for better stability, precision, speed, and controls while cost increases are kept in check.

By defining the critical metrological attributes in the design of goniometers, one can assess the design and manufacturing processes involved to achieve high-accuracy, high-precision rotation circles. The angular absolute positioning error of goniometers was defined as the deviation from the target angle during forward and/or backward rotation. When the direction of rotation is changed, there is an inherent "inversion error," which is a parallel offset in position error. The reproducibility is its ability to repeat an angular target position over several cycles. This includes bidirectional rotation. For single rotation circles, the errors defined are the axial motion error, the wobble error, which defines the plane's angular error perpendicular to the axis during rotation, and eccentricity which defines the circumferential trajectory error of the circle. For multi-axis rotation systems, the perpendicularity and parallelism errors among the rotation circle axes define the sphere of confusion. This is the locus of points summing all perpendicular and parallelism errors from each axis during rotation.

The manufacturing processes must suit the attributes defined above. However all processes (lathe tooling, milling, grinding, gear machining, coating) have tolerance limits and are influenced by several factors. These factors include machine thermal expansion from friction and motors, elastic deformation resulting from forces and torques acting on the workpiece during processing, mechanical vibration, and workpiece alignment. In one example, the periodic error of rotation is attributed to the workpiece clamping and the error of the lathe bearing. By applying compensation techniques, the processes can reduce the effects of these factors.

Proper manufacture of the worm gear system is the most important factor in achieving high performance in absolute accuracy, reproducibility, and reduction of inversion error. Fixturing the workpiece on the machine tool and tool precision can affect the overall performance. In addition, by controlling the pitch error of the gears to 1-2 μm , the angular accuracy achieved can be better than 0.7 arc-seconds for larger diameter circles.

The performance of the goniometers is influenced by temperature changes during operation. Each rotation cycle (forwards and backwards) causes a gradual shift in the inversion error as a result of temperature changes in the gear system. The counterbalancing of the precision worm-gear system is critical for achieving accuracy requirements. Counterbalancing maintains proper contact and force transfer between the gear teeth in the worm-gear system. Exceeding the design load and torque specifications can result in performance loss through high friction and possible damage.

The future of goniometer design and manufacture will involve the following: new materials and technologies; improved tool, measurement, and error compensation

systems: improved fitting of low tolerance parts; and reduction of human factors by maintaining highly skilled machine operators. In addition, systems can be improved by adapting them to specific applications in their operating environment.

Kevin D'Amico from X-ray Analytics, Ltd. made a general presentation on behalf of Kohzu Seiki Co. Ltd., regarding commercial monochromators for third-generation x-ray sources. The characteristics of the radiation produced by third-generation synchrotron radiation sources present technical challenges for the design of beamline optics. The high total power, high peak power, and brilliance of the radiation and the higher energy range place demands on all the optical elements. Brilliance affects angular stability. Power and power density impact cooling and cooling management. Energy range necessitates longer crystal travel putting a burden on crystal mounts and horizontal offsets for more challenging stability problems. Energy range further affects design and material selection for higher radiation resistance. One aspect of the hard x-ray optic performance that has been substantially left to the commercial segment of the synchrotron radiation community is the design and fabrication of the mechanics of the monochromators. Mechanical stability requires careful antivibration (jitter) packaging in the assembly as well as good understanding of the coolant and structure interactions. Additionally roll, pitch, and yaw motion designs should be carefully considered. D'Amico listed the common requirements of all monochromator users today to be: a stable fixed exit; cryogenic or gallium cooling; arc-second level stability in motions; a minimum of non-UHV components; precision encoders, and the availability of a large number of internal adjustments packaged at a reasonable cost. He explained these with a variety of examples of sample devices from the ESRF and Spring-8.

Richard Hewitt (with coauthor A.S.-Bommannavar) from Exxon Research (CMC CAT) gave a presentation on a versatile double-crystal monochromator (DCM) system for a water-cooled diamond or LN₂-cooled silicon crystal (see Fig. 1). This transmitting-type unique monochromator design offers a general purpose mount that is independent of the crystal system used for the energy selection. It takes advantage of the availability of modern synchronous motor technology with integral encoders and high precision bearings to achieve high precision, high reproducibility, and rapid setting. The mechanism is based on synchronous motors that generate the theta motion about the surface center of the first crystal and two linear motions of the second crystal perpendicular and parallel to the first crystal surface. The engineering of the cooled crystal mount exploits modern manufacturing technologies such as internal EDM'ing and new brazing techniques to achieve no coolant/vacuum joints for UHV operations. A similarly configured mount is used to achieve water-cooled diamond and LN₂-cooled Si crystals. The design separates the motion mechanism from the crystal vacuum chamber via a specially engineered vacuum "conductance limiting plate" thus reducing the expensive UHV needs. A two order of pressure difference is maintainable between the chambers.

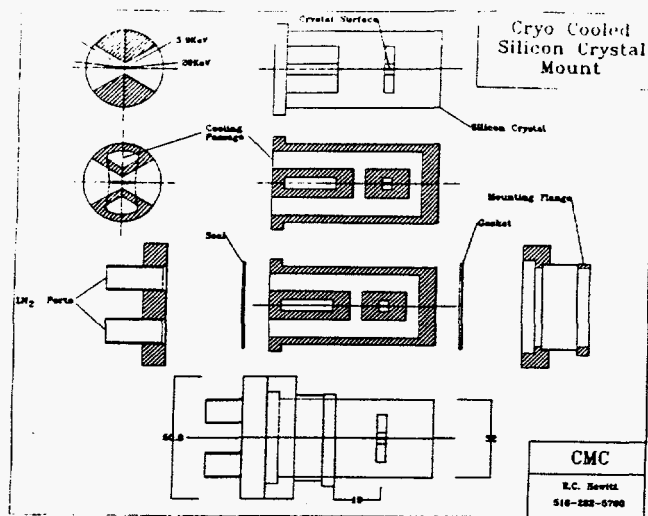


FIG. 1 Cryogenically cooled silicon crystal monochrometer - crystal holder design.

The synthetic single crystal diamond from Sumitomo is $0.5 \times 3.5 \times 7 \text{ mm}^3$. When inserted and brazed to a water-cooled mount, the useful area of the crystal becomes $2.5 \times 7 \text{ mm}^2$. In the current design, the diamond crystal was analyzed to withstand 120 W/mm^2 (17 W/mm^2 absorbed) with maximum absorbed total power of 68 W at 4.2 KeV , 30 meter from the APS undulator A source. In rocking curve studies and for a C $\langle 111 \rangle$ crystal, the Darwin width at 8 KeV was measured to be 6.9 arcsec against the theoretical 5.4 arcsec . C $\langle 111 \rangle$ is designed to operate in the $4 \text{ to } 13 \text{ KeV}$ energy range. This DCM features an independent theta drive for the two crystals. The center of rotation for each crystal is about the vertical center of line on the surface of the crystals. The second crystal is translated parallel to the incident beam direction of the first crystal to achieve a one inch fixed exit offset.

The LN₂-cooled Si $\langle 111 \rangle$ crystal is $0.6 \times 4 \times 20 \text{ mm}^3$ with a $2.5 \times 3.7 \text{ mm}^2$ active area. The Darwin width at 8 KeV is calculated to be 7.1 arcsec . Likewise it is designed to accept 120 W/mm^2 heat flux (36 W/mm^2 absorbed) with a maximum absorbed total power of 243 W . Si $\langle 111 \rangle$ is designed to operate in the $3 \text{ to } 20 \text{ KeV}$ energy range. This DCM features a common theta drive for both crystals. The second crystal is a long one to eliminate one translation. The first crystal is rigidly mounted to the common theta plate with the surface of the crystal on the axis of the rotation. The second crystal is translated perpendicular to the first crystal surface to achieve a fixed one inch vertical offset upward.

The next two talks in the morning program involved beam stability, mechanical stability, and the susceptibility of the x-ray beam position monitors (XBPM) to insertion-device gap changes. These problems have been observed and reported both by ALS and ESRF researchers (1 and 2). The bending magnet, contamination on the insertion device XBPM at low energies has been shown to be a considerable source of error. Tony Warwick described the ALS practices on such problems. The shadowing effect by the upstream XBPM blades are avoided in the usual manner of rotating the downstream XBPM blades with

respect to the upstream ones. The upstream XBPM has a pair of up and down blades. The downstream XBPM has four blades rotated at 45 degrees . The Glidcop blades penetrate into the $1/\gamma$ zone far enough to generate a robust photoemission signal but not far enough to disturb the diffraction-limited undulator central zone. The robust signal makes any effect of the weaker signal resulting from bending magnet contamination negligible. The blades are biased to $+75 \text{ V}$. Both the electronic stability and the mechanical stability of the XBPM systems have been assured. However, a "beam shift" registers a false beam position in the vertical blades. These blades have been found to be sensitive to the changing undulator gap because, with the change, the geometric pattern of the undulator beam illumination on the detector changes. As such, the blades "see" this as a "beam shift" registering a false beam position in the vertical. This phenomenon has been observed and verified in studies with XBPMs at both the ALS and ESRF. Warwick explained that, while this problem could be handled through an extensive corrective software in the XBPM signal processing programs, it remains a nagging problem.

The XBPM signal was further found to be sensitive to the undulator gap closing in the neighboring straight section. Dynamic closed orbit compensation was applied via a look-up table to correct the orbit position. With the orbit compensation, the resulting beam motion was reduced from 200 microns to 20 microns over an undulator gap variation between $200 \text{ to } 23 \text{ mm}$.

Deming Shu (with coauthors Juan Barraza, Tuncer M. Kuzay, and Mohan Ramanathan) from the APS presented a summary of the XBPM design development and performance data at the APS. The APS-developed XBPMs for the powerful white photon beam from undulator A use metal-coated blades made of chemical vapor deposition (CVD) synthetic diamond. The metallization causes the photoemission current, and the base material diamond provides the structural stiffness and the high heat dissipation under extreme heat load and flux. Two types of diamond blades have been developed. One is designed and configured like a conventional XBPM blade in which the beam hits the blade on edge. The other is called a transmitting-type (TBPM), in which the beam passes through a metallized or a patterned blade at right angle, and most of the x-rays are transmitted through the blade with a small fraction of the lower energy hard x-rays absorbed to cause the photoemission signal. The latter design is very versatile and can be used, depending on the metallized pattern and configuration, as an integrated XBPM, area monitor, window, flux detector, and beam profiler (Fig. 2). Prototypes of such devices have been built by the APS and successfully tested at CHESS and at the NSLS. Now a variety of ID front ends at the APS have these monitors both in the XBPM and TBPM forms. Also, special electronics have been designed and built for them. These have been recently tested for performance during commissioning studies at the APS. So far they have performed very well during the injected or stored beam modes of operation. Fig. 3 shows the normalized blade signal from a CVD diamond blade XBPM in the 1-ID front end at a modest 0.44-mA storage ring current. The special preamplifier and the preamplifier

controller with analog signal digitizer units are also designed in house. The 16-bit preamplifier has a six decade auto range in gain and has ± 0.1 nanoamp signal sensitivity. The mechanical stability of the XBPM supports and stages has been measured to be ± 0.2 micron. The blades are configured to avoid shadowing. In the ID front ends, the upstream XBPM has two pairs of vertically disposed blades, while the downstream one has two vertical and two horizontal blades. The horizontal blades are tilted and displaced slightly to avoid the particular contamination from the BM light.

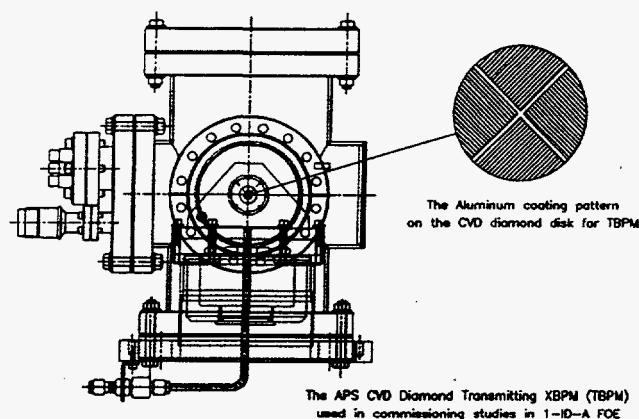


FIG. 2 The CVD diamond base transmitting photon beam position monitor.

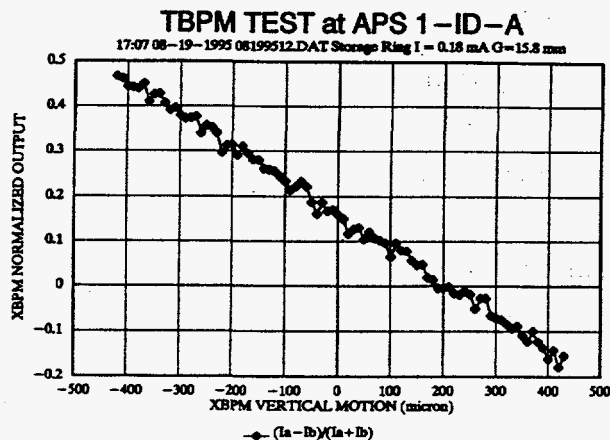


FIG. 3 Typical normalized signal for vertical beam position from the CVD diamond transmitting photon beam position monitor.

A recent novelty to the above electronics is the addition of a digital signal processor (DSP) and a system controller interface (SCI) to include an EEPROM chip, a CPU device, and D/A converter. The SCI receives the data on the ring current, ID magnet gap, and ID source characteristics. The normalized data from the XBPM is written on the EEPROM in a series of rapidly scanned calibration runs. Therefore a good data bank is created in the EEPROM for the correct beam center at varying gap, current, and the ID characteristics. This allows the XBPM to have memory for changing conditions. Hence it is called a smart

beam position monitor (SBPM). A prototype SBPM has been successfully tested using a PC in place of a controller CPU unit. A real unit is in the process of development and will be available for tests within about six months. It is expected that such a calibrated XBPM with memory will resolve the issues discussed in Warwick's presentation regarding varying gap and energy vulnerability of XBPMs.

II. THE AFTERNOON SESSION

The afternoon session started with Tom Swain's presentation on the development at the ALS of high performance Glidcop photon shutters as a general purpose component. Design constraints were UHV reliability, low cost, and implementation (installation) ease. The design was an extension of the highly effective microchannel-cooling concept extended to macrochannels for manufacturing ease and brazing feasibility of the two-part assembly. The 0.5-mm-wide coolant channels were cut into the Glidcop face plate using a carbide milling tool and with a 6:1 aspect ratio using a CNC milling machine. Full depth cuts were made at a 6 cm/min cutting rate. The mating back plate houses the air guard channels and the supply return manifold for the DI water. Then the face plate and the back plate were brazed using 0.002-inch-thick 50/50 gold-copper braze foil in a vacuum furnace. This assembly is said to be twice as effective in removing heat as any previously designed ALS absorber.

The next talk by T. Kuzay (coauthor-M. Sözen) was on the use of conductive porous media as a means to enhance heat transfer in beamline components subject to high heat load and high heat flux. This method was introduced at the APS and is used extensively in fixed mask, photon shutter, and slit cooling with single-phase water, as well as, recently, with LN₂, cooling of optics. For the porous media, copper mesh is used. This technique of heat transfer enhancement is very effective at the expense of a tolerable pressure drop; it is jitter-free and requires only a modest amount of deionized water flow. Copper and deionized water are very compatible, showing no corrosion effects in the long term. At the APS, a design goal has been to achieve an enhanced heat transfer coefficient of 3 W/cm²K in the cooling channels using approximately a 5 l/min water flow rate through the standard 9-mm-diameter holes using 80 percent porous media. The copper mesh is brazed to the copper channel surfaces for assured cooling efficiency. At the APS a large amount of experimental data was generated on the porous media heat transfer. The presentation by Kuzay explained the recent analytical work concerning the enhancement process so that these systems can be optimized with respect to the mesh fiber diameter and porosity. The complex analytical formulation is able to predict were the experimental APS data on surface temperature, pressure drop, and spatial and averaged heat transfer coefficients.

The model was recently extended to cryogenic cooling of optics using such bonded copper porous media. The subcooled LN₂ was driven to subcooled boiling. The analytical treatment of this problem ran into a snag because of lack of theoretical understanding of boiling heat transfer.

No correlations exist in subcooled boiling to model bubble formation, detachment, and burst. Hence at this stage, we were forced to use some scoping studies with experimental boiling heat transfer data with conductive mesh with cryogenics. It is well established that the porous media does not support nucleate boiling. The scant literature on conductive heat transfer with meshes without boiling suggests a 2.5 to 3-fold enhancement over plain tube boiling heat transfer. Our analytical model was applied to silicon optics built more like an APS front-end photon shutter (several cooling holes with copper mesh) placed at 30 meters from the source with the beam from APS undulator A (6 kW power with a maximum of $8.2\text{W}/\text{mm}^2$ surface heat flux). Enveloping correlative work concluded that such an optics can be cooled with LN2 in subcooled fashion at LN2 flow rates over 10 l/s.

In the next presentation, Karl Smolenski talked about the manufacturing and operational experience at CHESS on windows/filters. His presentation covered components on the CHESS F Wiggler Line both during previous operations at 100 mA and 5.3 GeV and since the recent upgrade in November 1994. The upgrade increased the positron beam current to 150 mA with plans to go 250 mA shortly in November 1995. The full power is 8.3 kW. To meet the heat load, the line contains one highly oriented graphite filter (HOPG) and two beryllium windows, each 250 micron. About 1.1 kW power is absorbed in the graphite filter with each Be window absorbing about 70 W. While the HOPG is a thermally excellent material, it is brittle and easily damaged in handling. In the CHESS experiments, it is brazed to a cooled copper mask. Wetting of HOPG was aided with the addition of 5% Ti with TiCuSil or CuSil-ABA or CerameTil 721. In the recent tests with high current operations, the IR camera measurements indicated filter centerline temperatures in excess of 800°C at 250mA operations. Due to cracks and delamination, the HOPG filter actually results in half of its published thermal conductivity value. However no further deterioration in the surface structure was observed. It was concluded that free/flexible or "dome type" window configurations should be beneficial in reducing stresses with the fixed/brazed filters. Alternatively compliant braze layers can be utilized or high conductivity carbon fiber curtain filters can be considered.

The Cornell vacuum was never compromised by a window failure with the double-window configuration. It has been established that, at CHESS and at 100 mA operations, the windows on the 24-pole wiggler line protected by a pyrolytic graphite filter last about 6 months, corresponding roughly to 4000 thermal cycles. Visible surface deformation precedes the failure. Hence visible periodic inspection may allow replacement before failure. However with the use of a water-cooled, brazed HOPG filter, the life of the Be windows was extended very substantially. Such a beamline has shown no noticeable reduction in the photon throughput since December 1992.

A follow up talk was given by Zhibi Wang of the APS on his recent experience at HASYLAB on the beamline component analysis with the PETRA conversion. Most of the beamline component analyses were done using XRAP (X-Ray Analysis Package). XRAP is an ANL-developed code

that unifies source, photon/material interactions, thermal/stress analysis with postscript file output for data output or a friendly graphics interface based on the X-Window Motif library.

Wang focused mostly on his work with the filter/window analysis of the PETRA undulator beamline Large. The PETRA undulator at HASYLAB, Germany, is a hard x-ray machine that is capable of delivering brilliant radiation in the energy range from 20 to about 200 keV at a maximum beam energy of 12 GeV. With a deflection parameter, $K = 2.49$, the total radiated power can be as high as 14.7 kW. As such, the filter and window design has become a challenging engineering problem. In order to reduce the low energy photons for the downstream beamline optics, filters are stacked from low-Z to high-Z in progression of C, Be, Al, Cu, Si, and Fe. In a sample case study, the throughput power is reduced to 1.33 kW with most of the power being absorbed in the metallic filters. Filters were optimized in design and correct order of stacking for reliability. The analyses were checked against more conventional packages including ANSYS for the highly nonlinear thermo-structural calculations. XRAP proved to be a useful, sophisticated, and accurate new tool that is drastically needed in the complex and precise analysis of beamline components in modern hard x-ray synchrotron facilities with very powerful beams.

III. OPEN FORUM

The part of the program summarized above concluded the planned workshop presentations. The final hour of the program was an open forum for discussion about subjects such as design for precision motions in optical mounts, smart filters, and the filter/window failure detection techniques. Time only allowed the first two subjects to be covered with discussion leaders Juan Barraza and Deming Shu from the APS, respectively.

Juan Barraza explained the principles of the APS kinematic mount designs using a cone, flat and groove (Fig. 4). These mounts have been extensively exploited in all component motions from front-end components to XBPMs to optical tables, slits, and mirror mounts both as supports as well as individual positioning stages. These kinematic mounts have been designed in three categories for coarse, medium, and precision movement and adjustment controls. Sample cases included XBPM stages that have proven 1-micron repeatability and 0.1-0.2 micron resolution under a load capacity of 90 kg. Trajectory is controlled to 10 microradian in 5-mm travel. In optical tables, a load capacity up to 454 kg (1000 pounds) was allowed with repeatability better than 50 microns in the open-loop mode. Typical resolution is better than 10 microns. Other participants brought up examples of the ALS-style six-strut mounts as well as providing a limited discussion on the hexapod style mounts. Consensus was such that the latter design, although very attractive and futuristic, has not developed yet to the required level of repeatability and resolution at a competitive cost basis.

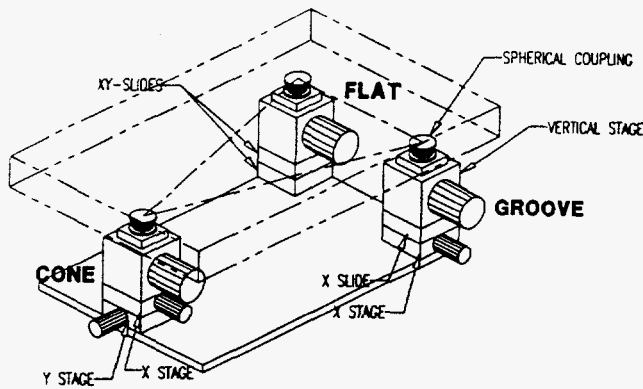


FIG. 4 The APS linematic mount design for universal use.

Deming Shu in the closing discussion explained the need for smart user filters at the APS. A conceptual configuration of such a filter is shown in Fig. 5. These filters have been designed to work with a variety of undulator/wiggler white beams. Typically they have a stack of five filters in a bank of four. Hence, in the current configuration, 625 filter permutations are available. Programmable logic controllers permit a protection system that can be programmed on an EEPROM for safe filter combinations commensurate with the storage-ring and the insertion-device variables. The smart filter is also tied in with the equipment protection system (EPS) for correct shutter enable/disable control. Any user-instigated power/filter mismatch can be automatically decided and not allowed. Fuzzy logic can be used to reduce the memory size and improve performance. Such a system is in the early stage of development at the APS.

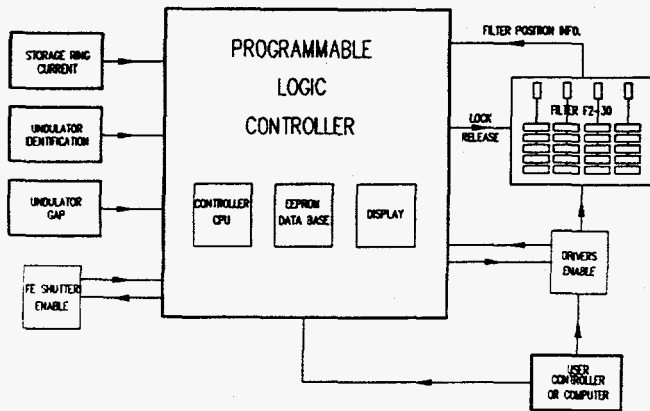


FIG. 5 Smart beamline filter configuration schematic.

ACKNOWLEDGMENTS

Cochairs T. Kuzay and T. Warwick would like to thank all the participants and the audience at this workshop which made it an interesting day of presentations and discussions at SRI'95 Conference. We thank Susan Picologlou for editing article. This work was supported by the U.S.

- ¹ G. Mülhaupt., Rev. Sci. Instrum. 66 (2), 1995.
- ² Tony Warwick et al., Rev. Sci. Instrum. 66 (2), 1995.
- ³ D. Shu et al., Nucl. Instrum Meth. in Physics Research A319 (1992) 56-62.
- ⁴ D. Shu et al., Nuclear Instrum. Meth. in Physics Research A 347 (1994) 577- 580.
- ⁵ D. Shu and T. M. Kuzay, A Smart Photon Beam Position Monitor System for the Advanced Photon Source Project," 1995. These proceedings.

The submitted manuscript has been authored by a contractor of the U.S. Government under contract No. W-31-109-ENG-38. Accordingly, the U. S. Government retains a nonexclusive, royalty-free license to publish or reproduce the published form of this contribution, or allow others to do so, for U. S. Government purposes.

DISCLAIMER

This report was prepared as an account of work sponsored by an agency of the United States Government. Neither the United States Government nor any agency thereof, nor any of their employees, makes any warranty, express or implied, or assumes any legal liability or responsibility for the accuracy, completeness, or usefulness of any information, apparatus, product, or process disclosed, or represents that its use would not infringe privately owned rights. Reference herein to any specific commercial product, process, or service by trade name, trademark, manufacturer, or otherwise does not necessarily constitute or imply its endorsement, recommendation, or favoring by the United States Government or any agency thereof. The views and opinions of authors expressed herein do not necessarily state or reflect those of the United States Government or any agency thereof.